

Nanoelectromechanical systems

# Nanodevice motion at microwave frequencies

It has been almost forgotten that the first computers envisaged by Charles Babbage in the early 1800s were mechanical<sup>1,2</sup> and not electronic, but the development of high-frequency nanoelectromechanical systems is now promising a range of new applications<sup>3</sup>, including sensitive mechanical charge detectors<sup>4</sup> and mechanical devices for high-frequency signal processing<sup>5</sup>, biological imaging<sup>6</sup> and quantum measurement<sup>7–9</sup>. Here we describe the construction of nanodevices that will operate with fundamental frequencies in the previously inaccessible microwave range (greater than 1 gigahertz). This achievement represents a significant advance in the quest for extremely high-frequency nanoelectromechanical systems.

Until now, it has not been possible to create mechanical devices that operate at extremely high frequencies, owing to the dual challenge of detecting tiny displacements (on the scale of femtometres) at microwave frequencies<sup>1,3</sup>. The characteristic frequency of nanoelectromechanical systems (NEMS) scales upwards with decreasing size, but their displacement (when operating linearly) and their electro-mechanical impedance both simultaneously scale downwards.

Two advances have been crucial to breaking the 1-GHz barrier in NEMS: the use of silicon carbide epilayers<sup>10</sup>, which are of comparable density but are significantly stiffer than the usual silicon<sup>11,12</sup>, and which allow higher frequencies to be attained for structures of similar geometry; and the development of balanced, high-frequency displacement transducers, which enable the ubiquitous passive embedding impedances that arise from electrical connections to the macroworld to be nulled<sup>13</sup> (if uncontrolled, these parasitic impedances overwhelm the electromechanical impedance of interest — the 'signal' — in ultrasmall NEMS).

We used 3C–SiC films that were grown hetero-epitaxially at atmospheric pressure by chemical-vapour deposition in an induction-heated reactor on 100-mm-diameter (100) Si wafers<sup>10</sup>. Device nanofabrication involves both optical and electron-beam lithography to define, respectively, large-area contact pads and submicrometre-scale, thin metallic-film masks with the device geometry. Pattern transfer to the 3C–SiC layer is achieved by an electron cyclotron resonance (ECR) plasma-etch step involving an NF<sub>3</sub>/O<sub>2</sub>/Ar mixture. The patterned 3C–SiC beams are then suspended above the underlying silicon substrate by using an isotropic NF<sub>3</sub>/Ar ECR etch. The metallic mask

(30 nm of aluminium, followed by 5 nm of titanium), deposited by e-beam evaporation and patterned by lift-off, remains on the beams and is used as the electrode for displacement transduction. The devices consist of two nominally identical, doubly clamped beams, roughly 1.1 μm long, 120 nm wide and 75 nm thick.

Each doubly clamped beam pair is positioned perpendicular to a strong magnetic field (3–8 tesla) *in vacuo* within a liquid-helium cryostat. Balanced magnetomotive detection is used<sup>13</sup>, when the driving frequency matches the fundamental frequency of the in-plane flexural mode for one of the beams, there is resonant enhancement of the induced electromotive force. This response is pre-amplified and characterized by a microwave-network analyser.

Fundamental mechanical resonances are detected at 1.014 GHz and 1.029 GHz for the two beams (Fig. 1). So far, quality factors attained above 1 GHz (about 500) are substantially lower than observed for NEMS in roughly the 100-MHz range (about 10<sup>4</sup>). Having ruled out factors such as electrical damping, we are investigating whether this stems from roughness in the initial SiC epilayers, and how such sources of acoustic loss in microwave NEMS can be minimized. Nonetheless, this step into the previously inaccessible domain of microwave-frequency mechanical excitations constitutes a milestone along the path to the many new applications offered by nanomechanical systems.

Xue Ming Henry Huang\*, Christian A. Zorman†, Mehran Mehregany†, Michael L. Roukes\*

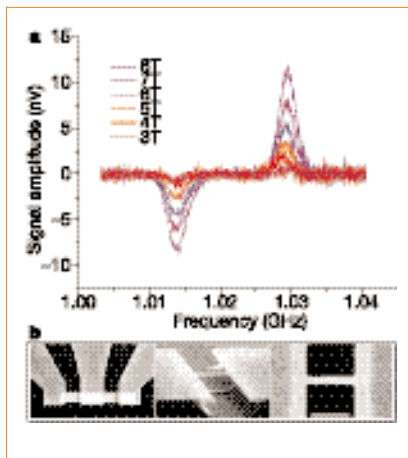


**Figure 1** Microwave-frequency nanomechanical devices. **a**, Fundamental flexural-mode resonant mechanical response at 1.014 and 1.029 GHz, detected at about 4.2 K from a pair of doubly clamped silicon carbide beams as a function of applied magnetic field (3–8 tesla). These devices are electrically connected within a balanced magnetomotive detection scheme<sup>12</sup>; each distinct resonance corresponds to excitation of one of the beams within the device. **b**, Scanning electron micrographs of a similar (slightly larger) pair of devices, with magnified views of a single resonant element. Scale bar, bottom right, 1 μm.

\*Condensed Matter Physics, California Institute of Technology 114-36, Pasadena, California 91125, USA  
e-mail: roukes@caltech.edu  
†Electrical Engineering and Computer Science, Case Western Reserve University, Cleveland, Ohio 44106, USA

- Roukes, M. L. *Sci. Am.* **285**, 48–57 (2001).
- Swade, D. *The Difference Engine: Charles Babbage and the Quest to Build the First Computer* (Viking-Penguin, New York, 2001).
- Roukes, M. L. *Phys. World* **14**, 25–31 (2001).
- Cleland, A. N. & Roukes, M. L. *Nature* **392**, 160–162 (1998).
- Nguyen, C. T.-C., Katehi, L. P. B. & Rebeiz, G. M. *Proc. IEEE* **86**, 1756–1768 (1998).
- Sidles, J. A. *et al. Rev. Mod. Phys.* **67**, 249–265 (1995).
- Cho, A. *Science* **299**, 36–37 (2003).
- Armour, A. D., Blencowe, M. P. & Schwab, K. C. *Phys. Rev. Lett.* **88**, 148301 (2002).
- Bocko, M. F. & Onofrio, R. *Rev. Mod. Phys.* **68**, 755–799 (1996).
- Yang, Y. T. *et al. Appl. Phys. Lett.* **78**, 162–164 (2001).
- Carr, D. W., Evoy, S., Sekarik, L., Craighead, H. G. & Parpia, J. M. *Appl. Phys. Lett.* **75**, 920–922 (1999).
- Clark, J. R., Hsu, W.-T. & Nguyen, C. T.-C. in *Technical Digest, IEEE Int. Electron Devices Meeting, San Francisco, California (11–13 December 2000)* 493–496 (2001).
- Ekinici, K. L., Yang, Y. T., Huang, X. M. H. & Roukes, M. L. *Appl. Phys. Lett.* **81**, 2253–2255 (2002).

Competing financial interests: declared none.

COMMUNICATIONS ARISING

Genomic function

# Rate of evolution and gene dispensability

Whether more dispensable genes evolve faster than less dispensable ones<sup>1</sup> is a contentious issue<sup>2–4</sup>. Comparing yeast and worm genes, Hirsh and Fraser<sup>3</sup> observe a gradual tendency for less dispensable genes (those that reduce the growth rate of yeast when knocked out) to have lower rates of protein evolution. Here we repeat their analysis using larger data sets and find no evidence that dispensability explains the variation in rates of protein evolution. Although Hirsh and Fraser provide a model to show why their result is to be expected, our analysis suggests that their model, which assumes among other things that no substitution is advantageous, cannot be generally applied.

To estimate the rate of evolution, Hirsh and Fraser used orthologues identified in the worm *Caenorhabditis elegans*. But using so distant a relative of the yeast *Saccharomyces cerevisiae* may have pitfalls. We have therefore repeated the analysis using *C. elegans* and three other closer relatives of *S. cerevisiae* (*S. bayanus*, *Candida albicans* and *Schizosaccharomyces pombe*). Unlike *Caenorhabditis*, for which the most recent common ancestor with yeast existed between 1.0 billion and 1.6 billion years ago, these three species are separated from *S. cerevisiae* by about 10 million, 140–310 million and 330–440 million years, respectively. New fitness data<sup>5</sup> enable complete genomes to be analysed using samples that

